A Minimal Model for the Helix−Coil Transition of Wormlike Polymers. Insights from Monte Carlo Simulations and Theoretical Implications

Vikas Varshney, Taner E. Dirama, Taner Z. Sen,† and Gustavo A. Carri*

The Maurice Morton Institute of Polymer Science, The University of Akron, Akron, Ohio 44325-3909

Received April 5, 2004; Revised Manuscript Received August 26, 2004

ABSTRACT: We present a geometric approach to the simulation of the helix−coil transition in wormlike polymers. Our approach has its foundations on a novel real-space realization of the concepts proposed by Zimm, Bragg, and other researchers. In our model, the polymer is treated as a freely rotating chain with hard-core repulsion between beads. The conformational state (helix or coil) of each bead is determined by the value of its torsion. If the difference between the torsion of a bead and the one of the perfect helix is less than a cutoff value, then the bead is part of a helical domain and carries a negative energy; otherwise, it is part of a random coil. In addition, interfaces between helical and random coil domains carry an energy penalty. We have simulated these concepts using the Wang−Landau algorithm where the density of states depends on two parameters: the number of beads in the helical state and the number of interfaces. In this article we show that these simple ideas can account for the cooperativity of the transition explicitly and capture the known conformational, configurational, and thermodynamic properties correctly. Moreover, these concepts have important theoretical implications since they lead naturally to a field-theoretic Hamiltonian of the Edwards' type that might be useful for problems of current experimental interest.

Introduction

The seminal discovery of α-helices and β-sheets by Pauling, Corey, and Branson[1] in 1951 motivated intense research in the field of secondary and tertiary structures of biopolymers. In particular, α-helices have been the subject of many experimental studies in the polymer science community where single polymers capable of adopting helical conformations, like polypeptides and chiral polyisocyanates, have been studied extensively.[2] The effects of solvent,[3] molecular weight,[2] chirality of the biopolymer[4] or solvent,[5] simple shear flow,[6] ions,[7] surfaces,[8] and other experimental parameters on the helix formation of single polymers have been studied and are topics of current experimental interest. These experimental studies have provided researchers with a good understanding of the helix−coil transition of single polymer chains.

Theoretical studies have also been developed to provide a framework for the understanding of the experimentally observed behaviors. Most of these studies are based on the traditional matrix method first proposed by Gibbs and DiMarzio,[9] Zimm and Bragg,[10] and Lifson and Roig.[11] Extensions of these concepts include extra features that allow them to describe solute effects,[12,13] polyelectrolytes,[14] copolymers,[13] helix induction by hydrogen-bonding chiral solvent molecules,[15] preferences for the N-cap, N1, N2, N3, and C-cap positions, capping motifs, helix dipoles, side-chain interactions, and 3_{10}-helix formation.[16] Of special interest are two recent studies done by Buhot and Halperin[17] and Tamashiro and Pincus[18] where they addressed the force−elongation behavior of homopolypeptides. For this purpose these researchers employed the theoretical approach originally formulated by Nagai where the traditional matrix method and the freely jointed chain model are combined to calculate real-space properties like the mean-square end-to-end distance.[19] Furthermore, Buhot and Halperin have also used the wormlike chain model in their calculations.[20] Alternative approaches to the helix−coil transition have also been developed. For example, Muthukumar[21] developed a statistical mechanics approach based on a novel field-theoretic method to study the helix−coil transition, among other physical phenomena, and Paoletti et al.[22] developed a fully thermodynamic approach to describe counterion condensation on a biopolyelectrolyte capable of a conformational transition between two different conformations.

The helix−coil transition of peptides has also attracted a lot of attention from the computer simulations perspective. Indeed, the increase in computational speed due to improvements in hardware and the development of very efficient algorithms have allowed researchers to run atomistic and coarse-grained Monte Carlo simulations of polymers with secondary structures using the multicanonical algorithm of Hansmann and Okamoto,[23] the algorithm originally developed by Wang and Landau[24] (as implemented by Rathore and de Pablo[25]) and other algorithms. These approaches to the problem are very powerful because they carry out a random walk on the energy surface and, in principle, are capable of capturing the thermodynamics of the different systems accurately. As a consequence of this, the aforementioned algorithms have proven to be very efficient in folding single peptides into α-helical structures.[26] Moreover, it is clear that these algorithms provide the best way to address the problem of helix formation at present. The only disadvantage is that the computational time needed to generate the flat energy histogram required by the algorithms increases rapidly with the number of states, putting many systems of current experimental and theoretical interest out of the reach of atomistic computer simulations.

† Present address: L. H. Baker Center for Bioinformatics and Biological Statistics, 112 Office and Laboratory Bldg., Iowa State University, Ames, IA 50011-3020.

* To whom any correspondence should be addressed. E-mail: gac@uakron.edu.

10.1021/ma049338u CCC: $27.50
Published on Web 10/09/2004

The increase in the number of states with increasing number of atoms implies that if we want to address the *general* behavior of many-chain systems of current interest like hydrogels of diblock copolypeptides[27] and networks of helix-forming polymers,[28] or the general behavior of charged or chiral many body-systems involving only one helical chain like a single helical polyelectrolyte with its counterions[22] and salt ions, or the induction of helical structures on a polymer due to hydrogen bonding of chiral and achiral molecules,[15] we must coarse-grain the description of the *polymer* as much as possible without losing the helical characteristics of the chain. The coarse-graining process decreases the total number of possible states by removing those states with characteristic length scales of the order of angstroms which are irrelevant for the large length scale behavior of the *polymer*. Therefore, it allows us to use the algorithms mentioned previously to study systems with more than one polymer or systems for which an explicit (coarse-grained) description of the counterions or solvent molecules is essential.

In this article we propose a minimal (coarse-grained) model that couples the helix−coil transition of polymers with the semiflexibility of the polymer backbone and study its conformational, configurational, and thermodynamics consequences. The simplicity of the model makes it very flexible because small additions to it should be able to describe the physical behaviors of more complex systems like the ones mentioned in the previous paragraph. The proposed model is a real-space realization of the traditional ideas of helix−coil transition theory.[9−11] Indeed, the bridging between the Ising-like concepts used in the traditional matrix treatments of helix−coil transition and the real-space helical structure is done using the geometrical concept of torsion of a curve which is employed to determine the conformation of each bead. Once the conformation of each bead is known for each configuration of the chain, the algorithm developed by Wang and Landau[24] as implemented by Rathore and de Pablo[25] is used to compute the density of states. Afterward, standard statistical mechanics formulas are employed to calculate the configurational, conformational, and thermodynamic properties of the model.

This article is organized as follows. In the next section, we present the conceptual foundations of the model and the simulation protocol. Special emphasis is put on the connections between the traditional concepts of helix−coil transition theory and the proposed model. The following section contains the results of our model and their discussion. In this section, we pay special attention to the comparison of our results with known results from other simulation, experimental, and theoretical studies. Toward the end, we explore the theoretical implications of our simulation study and propose a field-theoretic Hamiltonian of the Edwards' type that should describe the helix−coil transition of semiflexible polymers. Finally, we conclude this article with a summary of our results and the appropriate acknowledgments.

Model and Simulation Protocol

A. The Model. The success of the traditional methods and concepts of helix−coil transition theory in describing the experimental data quantitatively implies that our model must be constructed around these ideas. However, the main purpose of our model is to describe not only the conformational properties but also the configurational ones. Therefore, a real-space realization of the traditional concepts of helix−coil transition must be developed. This was originally stated by Lifson and Roig,[11] who started their model by considering the dihedral angles along a polypeptide chain. However, after developing a few concepts, they mapped this description of the polypeptide onto the traditional Ising-like concepts, thus losing the real-space *configurational* information (e.g., $\langle R_g^2 \rangle$) of the system.

In our model, we want to keep the structural information as well as capture the conformational properties correctly. Therefore, we start the construction of our model with the freely rotating chain model where the bond lengths and bond angles are constant. For simplicity, we consider only one bond angle and bond vector. This implies that each residue of the polypeptide chain is replaced by a bead. Clearly, this is not a strong limitation of the model since refinements can easily be constructed by replacing the different chemical groups of each residue by beads with different properties.

At this point a very pertinent question arises: how to couple the traditional concepts of helix−coil transition theory with the freely rotating chain model. To answer this question, we must remember that one of the most common molecular driving forces that stabilize the helical structure is hydrogen-bonding interactions between pairs of residues. To be more precise, the hydrogen-bonding interaction occurs between residues that are separated by two or three other residues along the polymer backbone. In order for this hydrogen bond to form, the distance between the pair of residues must be small. In other words, the residues between the hydrogen-bonding pair must be in very specific spatial positions such that the pair of residues can come close to each other and form the bond. This process implies a considerable amount of cooperativity along the polymer backbone. Our model must capture this cooperativity explicitly.

The work of Lifson and Roig[11] shows that the dihedral angles are crucial quantities for the description of the helix−coil transition. We also note that it would be very convenient to define a criterion that determines the conformational state of each bead based on dihedral angles because these angles can account for the cooperativity of the transition explicitly. This is a consequence of the fact that dihedral angles depend on the spatial locations of *four consecutive* beads along the polymer backbone. Therefore, the use of dihedral angles to determine the conformation of each bead is the correct way of bridging between the configurational and conformational properties of helical polymers.

A more robust *geometrical* quantity for the aforementioned criterion is the one of torsion of a curve. Imagine the bead representation of the polymer as the discrete version of a continuous, threadlike, representation of the chain; then the torsion of the curve is a well-defined mathematical quantity in both continuous and discrete representations of the polymer. Moreover, in the particular case of the discrete model, the torsion is related to *two consecutive* dihedral angles of the polymer. Equation 1 defines the torsion, called $\chi(x)$ hereafter, of a curve parametrized by the vectorial field $\mathbf{r}(x)$ which represents the polymer chain. "x" is the arc of length parameter that can take any value in the interval $[0,L]$, and L is the contour length of the polymer chain

$$\chi(x) = \frac{(\mathbf{r}'(x),\mathbf{r}''(x),\mathbf{r}'''(x))}{|[\mathbf{r}'(x),\mathbf{r}''(x)]|^2} \qquad (1)$$

where $\mathbf{r}'(x)$, $\mathbf{r}''(x)$, and $\mathbf{r}'''(x)$ are the first-, second-, and third-order derivatives of $\mathbf{r}(x)$, respectively. The square brackets and parenthesis indicate vectorial and scalar triple product (i.e., $(\mathbf{A},\mathbf{B},\mathbf{C}) = \mathbf{A}\cdot(\mathbf{B} \times \mathbf{C})$), respectively. This definition of torsion is also valid for the discrete representation of the polymer chain; the only difference is that the derivatives of the field must be approximated using finite differences. For example, the first-order derivative of the field on the ith bead is

$$\mathbf{r}'(i) \approx \frac{\mathbf{r}(i+1) - \mathbf{r}(i-1)}{2l_K} \tag{2}$$

where l_K is the bond (Kuhn) length. Similar expressions are also available for the second- and third-order derivatives.[29] The dependence on the third-order derivative implies that the torsion on the ith bead depends on the spatial locations of the beads $i-2$, $i-1$, i, $i+1$, and $i+2$. Consequently, the torsion can be calculated for beads 3 to $n-2$ where n is the total number of beads in the polymer chain.

Let us now use the concept of torsion as a criterion to determine the conformation (helix or coil) of each bead. For the sake of argument we assume that we know all the geometrical properties of the perfect helical state (i.e., the radius of the helix and its pitch). This information can be translated into the curvature and torsion of the helix using standard formulas.[30] The curvature determines the bond angle which is fixed in the freely rotating chain model. The torsion, which is governed by two consecutive dihedral angles, is the torsion of the perfect helix. Consequently, we define the following criterion: "a bead has a helical conformation if the value of its torsion, as defined by eq 1, differs from the torsion of the perfect helix, χ_{helix}, by less than a certain cutoff value, χ_{cutoff}". If the criterion is satisfied, then the helical bead carries a negative enthalpy, called C, which stabilizes the helical conformation; otherwise, the bead is in the random coil state which is the reference state. The enthalpic parameter C is related to the standard parameter s of the helix−coil transition theory[10]

$$s = \exp(-\Delta F/k_B T) \tag{3}$$

as follows: $\Delta F = C - T\Delta S$. Thus, C represents the enthalpic contribution that arises from the formation of a hydrogen bond. Furthermore, ΔS is the decrease in entropy due to the formation of the new hydrogen bond. In our model, this decrease in entropy is introduced by the freely rotating chain (FRC) model and the constraints on the dihedral angles. In addition, both parameters C and ΔS are negative. It should be noted that there are experimental situations where both parameters C and ΔS are found to be positive. This is a solvent effect. In these cases, the helical structure is stabilized at high temperatures.[10] Positive values of the parameter C include the heat of desorption of a solvent molecule from a random segment of the chain when the latter adopts the helical conformation. On the other hand, positive ΔS is due to the increase in solvent entropy which overrides the decrease in chain entropy upon formation of the helix. In our model, there is no solvent; therefore, the stabilization of the helical state occurs at low temperature, implying negative values for the parameters C and ΔS. It can be easily deduced from the equation that ΔF is 0 when $T = T_m$ $(= C/\Delta S)$. This temperature is known as the melting temperature and is characteristic of helix melting. For values of T less than T_m, ΔF is negative, i.e., $s > 1$. In this regime, the formation of hydrogen bonds is preferred, and hence, helices are favored. On the other hand, when T is larger than T_m, ΔF is positive, i.e., $s < 1$. Under this condition the random coil conformation is favored and the helices melt. Another traditional parameter used in helix−coil transition theory is the penalty for the formation of interfaces between random coil and helical domains.[10] This penalty is associated with the parameter "σ", which is a Boltzmann weight and is related to the initiation of a new helix. The fact that the polymer sacrifices the configurational entropy of three consecutive residues for the formation of the first hydrogen bond makes the initiation of the new helix an improbable event when compared to the propagation of an existing helix where a new hydrogen bond is generated at the cost of the conformational entropy of only one residue. Consequently, the Boltzmann weight "σ" is always less than unity; generally, it is of the order of 10^{-2}−10^{-4}. In our model, we incorporated this parameter as an energy penalty for the formation of interfaces and is denoted as "η", which is positive by definition; therefore, it destabilizes the formation of interfaces. The parameter "η" together with the FRC model and the constraints on the dihedral angles determine the final value of the parameter "σ" of the traditional helix−coil transition theories. For simplicity, we assume that C and η are constants. In the next subsection we explain how to solve these ideas using the Monte Carlo algorithm of Wang and Landau.[24]

B. Simulation Methodology. We used the freely rotating chain model where the bond length was set equal to 1.53 (in arbitrary units) and the bond angle was 109.3°. Both parameters were kept constant during the simulation. The concept of torsion, as explained in the previous subsection, was used to determine the conformation of each bead for each configuration of the chain. The torsion of the perfect helix was chosen as 0.87, which corresponds to two consecutive dihedral angles of +90°, and the chosen cutoff value was 0.001. The values for the bond length, bond angle, and perfect torsion were chosen arbitrarily for convenience and not with the purpose of mimicking the properties of any known polymer in particular. However, it is important to note that, although a different set of values of the parameters does not affect the thermodynamics of the transition, it does affect the behavior of the configurational properties to some extent. For example, if the value of the perfect torsion is chosen such that it corresponds to a very low value of the translation per residue (l_1) with respect to Kuhn length (l_0) (*unlike in our simulations*), then the plot of $\langle R_g^2 \rangle$ as a function of the helical content is expected to show a minimum for low values of the initiation parameter due to the formation of short helical domains.[19]

The initial configuration of the polymer chain was generated randomly. The first bead was placed at origin and did not move during the simulation. The initial position of the second bead was along X-axis and at distance equal to 1.53 from the origin. The third bead was located on the $X-Y$ plane so that the bond angle was 109.3°, and moreover, the second bond had a positive projection onto the Y-axis. The positions of all other beads were computed using random dihedral angles with respect to previous three beads. These

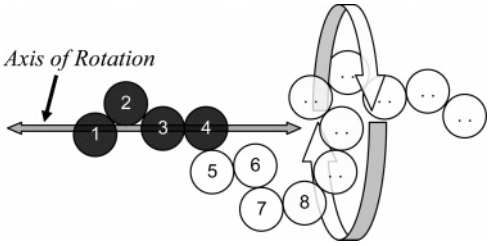

Figure 1. Graphical representation of the pivot move.

angles were taken from a prescribed finite set of 64 possible values, $\phi = 90 + (m\pi/32)$, where ϕ represents the dihedral angle and m varies from 0 to 63. This was done for the purpose of having a finite estimate for the density of states as explained below.

Pivot moves were used to change the configuration of the chain. In the pivot move, the ith bead is selected randomly and the rest of the polymer (beads $i + 1$ to n) is rotated around the bond between beads $i - 1$ and i by a randomly chosen angle. Figure 1 depicts the move.

The Monte Carlo algorithm chosen was the one recently developed by Wang and Landau.[24] This algorithm generates a random walk in energy space with a probability proportional to the reciprocal of the density of states, $g(E)$, and leads to a flat energy histogram. Analogous to the multicanonical algorithm,[23] this method has the advantage of escaping local energy minima and exploring the free energy landscape efficiently which, in turn, leads to an accurate estimate of the density of states, $g(E)$, for any system of interest. Once the density of states is known, all the statistical properties can be evaluated at any temperature using standard formulas from statistical mechanics. Another striking feature of this algorithm is the fact that it is independent of temperature, which makes it very useful to study a broad variety of systems. Although de Pablo and coworkers have pointed out two important limitations of the Wang−Landau sampling related to its accuracy,[31] it gave very good estimates for the density of states of our model.

In this article, we employ a two-dimensional version of the Wang−Landau algorithm to explore energy (arising from *the number of beads in the helical conformation*) and *interface* spaces which are required for the estimation of the density of states. Analogous to the energy space, where the energy adopts discrete values ranging from 0 to $(n - 4)C$ in steps of$C$, the *interface* space has the information about the number of interfaces between random coil and helical domains in all configurations of the polymer chain. So, in our case, the density of states is a function of two variables: the energy E due to the beads in the helical state and the number of interfaces present in the polymer, N_s.

Let us now review the Wang−Landau[24] algorithm, which is the starting point for this study. At the beginning of the simulation, the density of states $g(E,N_s)$, which is unknown a priori, is initialized to one for all possible values of the energy and number of interfaces. The random walk is then started by changing the configuration of the polymer. The transition probability for switching the polymer configuration from $\{E_i,N_{si}\}$ to $\{E_f,N_{sf}\}$ is

$$\text{Prob}(E_i,N_{si} \rightarrow E_f,N_{sf}) = \min\left(1, \frac{g(E_i,N_{si})}{g(E_f,N_{sf})}\right) \quad (4)$$

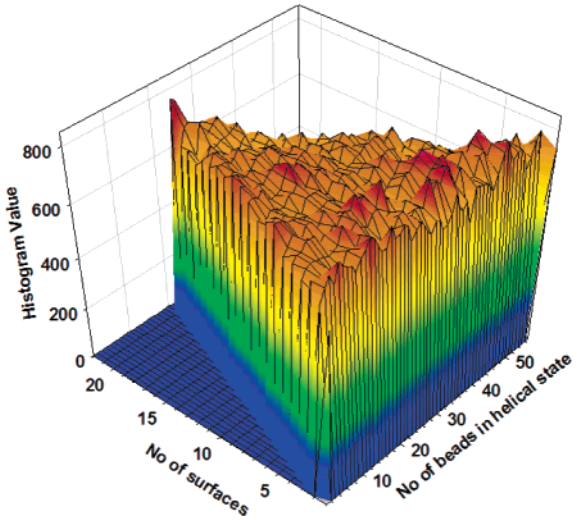

Figure 2. Typical energy histogram obtained from Wang and Landau's sampling.

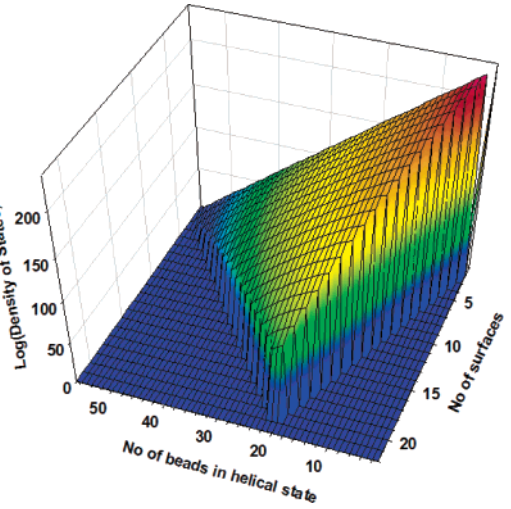

Figure 3. Typical density of states obtained from Wang and Landau's sampling.

Each time a move is accepted, the density of states of the new configuration is updated by multiplying the existing value by a modification factor f, i.e., $g(E, N_s) \rightarrow g(E, N_s) \times f$. However, if the move is rejected, then the density of states of the old configuration is updated. This modification allows the random walk to explore the energy and interface spaces quickly and efficiently. The starting value of f was taken to be e^1 (=2.71828), as recommended by Wang and Landau. After a move is completed, the corresponding histogram $H(E, N_s)$ is updated along with the modification of the density of states. Once the histogram is "flat" within some tolerance, the value of f is modified using Wang and Landau's recommendation $f_{new} = \sqrt{f_{old}}$. At this point, the histogram is reset to zero, and the above procedure is started again with the updated modification factor. This procedure is repeated until the value of f is very close to 1. We stopped our simulations when $f - 1$ became smaller than 10^{-7}. Figures 2 and 3 show typical results obtained for our model using Wang and Landau's algorithm. These figures were obtained for a chain with 60 beads.

Using the density of states, various conformational, configurational, and thermodynamic quantities were calculated using standard formulas from statistical

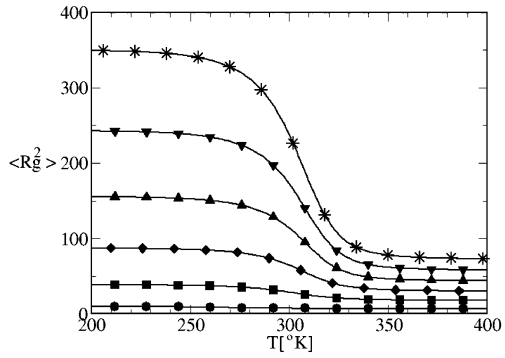

Figure 4. Plot of $\langle R_g^2 \rangle$ as a function of temperature for different chain lengths. The values of the parameters are $C = -1300$ K and $\eta = 0$ K. (●) $n = 10$, (■) $n = 20$, (◆) $n = 30$, (▲) $n = 40$, (▼) $n = 50$, (*) $n = 60$.

mechanics. The mathematical expressions for the canonical partition function, Helmholtz free energy, internal energy, entropy, and heat capacity are

$$Z(T,\eta) = \sum_{E,N_s} g(E,N_s) e^{-\beta(E+N_s\times\eta)} \tag{5}$$

$$F(T,\eta) = -T \ln\left(\sum_{E,N_s} g(E,N_s) e^{-\beta(E+N_s\times\eta)}\right) \tag{6}$$

$$U(T,\eta) = \langle E \rangle_T = \frac{\sum_{E,N_s} (E + N_s \times \eta) g(E, N_s) e^{-\beta(E+N_s\times\eta)}}{\sum_{E,N_s} g(E, N_s) e^{-\beta(E+N_s\times\eta)}} \tag{7}$$

$$S(T,\eta) = \frac{U(T,\eta) - F(T,\eta)}{T} \tag{8}$$

$$Cv(T,\eta) = \frac{\langle E^2 \rangle_T - \langle E \rangle_T^{\,2}}{T^2} \tag{9}$$

where $F(T,\eta)$, $U(T,\eta)$, $S(T,\eta)$, and $Cv(T,\eta)$ are in units of Boltzmann's constant, k_B. Apart from these thermodynamic quantities, the ensemble average of any other quantity of interest can also be calculated using following equation:

$$\langle A(T,\eta) \rangle = \frac{\sum_{E,N_s} A(E,N_s) g(E,N_s) e^{-\beta(E+N_s\times\eta)}}{\sum_{E,N_s} g(E,N_s) e^{-\beta(E+N_s\times\eta)}} \tag{10}$$

Results and Discussion

A. Configurational Properties. We start analyzing the consequences of our minimal model by considering the configurational properties of the polymer. For the purpose of clarity, we set the parameter η to zero for now and leave the study of the interfacial penalty for the last part of this section. Figure 4 shows the behavior of the mean-square radius of gyration, $\langle R_g^2 \rangle$, as a function of temperature (in K) for different chain lengths. The value of the parameter C ($= -1300$ K) was chosen in such a way that the helix−coil transition occurs around room temperature. This figure clearly shows the existence of two different regimes. At low

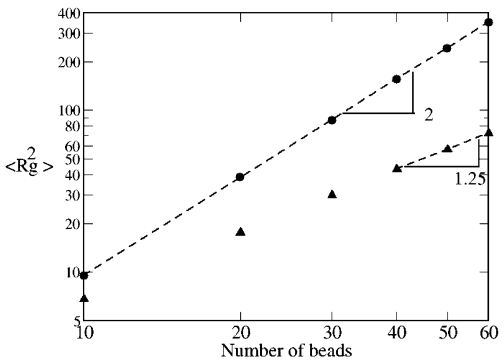

Figure 5. Plot of $\langle R_g^2 \rangle$ as a function of the number of beads for low and high temperatures. The values of the parameters are $C = -1300$ K and $\eta = 0$ K. (●) Low temperatures, (▲) high temperatures.

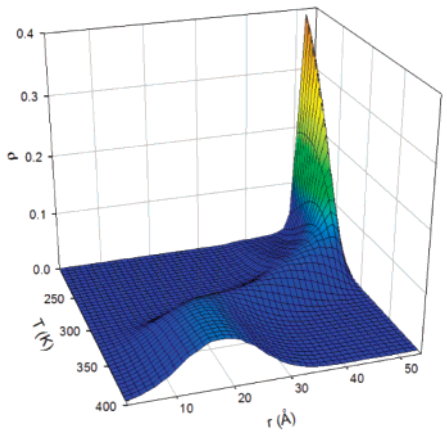

Figure 6. Plot of the radial distribution function for the chain ends as a function of the end-to-end distance and temperature. The values of the parameters are $C = -1300$ K and $\eta = 0$ K.

temperatures, the model predicts an extended configuration for the polymer chain which is consistent with the formation of a helical (rodlike) structure. At high temperatures, the polymer decreases its size which supports the existence of a random coil conformation.

One way to confirm the presence of these two conformations is to analyze the power law behavior of $\langle R_g^2 \rangle$ as a function of chain length (cl) at low and high temperatures. This has been plotted in Figure 5 on a double-logarithmic plot. This figure clearly shows that the $\langle R_g^2 \rangle$ scales as cl^2 at low temperatures, indicating the presence of an extended, rodlike structure, and as $cl^{1.25}$ at high temperatures, indicating the existence of a random coil conformation with excluded-volume interactions. The small deviation from 1.17 at high temperatures indicates that our polymer is still short. In other words, the chain length is not large enough to be in the self-avoiding walk regime. To elaborate on this conformational structure a little further, we plotted the radial distribution function (probability of finding the polymer with an end-to-end distance equal to r) for the chain ends as a function of the end-to-end distance r and temperature in kelvin. Figure 6 shows this plot for a polymer with 50 beads. Observe the similarities between this plot and the same plot for wormlike chains[32] where temperature is replaced by the persistence length of the polymer. At high temperatures, the radial distribution function shows a shallow peak for small values of the end-to-end distance which is typical of polymers with low degrees of stiffness (random coils). However, as the temperature is reduced, the model

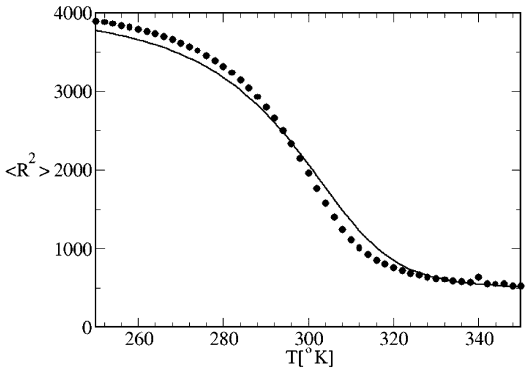

Figure 7. Plot of $\langle R_g^2 \rangle$ as a function of temperature (in K) for a chain with 60 beads: line (our result), circles (Nagai's model.).

predicts a shift in the peak to larger values of the end-to-end distance. Using the similarities with the wormlike chain model, we can say that the polymer chain becomes stiffer as the temperature is reduced.

All the aforementioned configurational properties prove that the model predicts the existence of a rigid polymer at low temperatures. The helical conformation is one possible structure, but there might be others. Thus, the definite proof that our minimal model predicts a helical structure at low temperatures comes from the Landau−Wang sampling which allowed us to determine the "ground" state of the system. This state turned out to be a perfect helix. Thus, we conclude that our model is predicting the transition from a helix to a coil as the temperature is increased.

For the purpose of making our discussion of the configurational properties more balanced and objective, it is appropriate that we compare our results with the ones obtained using one of the well-established theories of helix−coil transition. We chose the model developed by Nagai.[19] Figure 7 shows a quantitative comparison between our result for $\langle R^2 \rangle$ and the one obtained from Nagai's model for a chain with 60 beads. The values of the parameters of Nagai's model are $l_1 = 3$, $l_0 = 2.5$, $n = 60$, and $\alpha = 0.25$. The value of the enthalpy used in the expression for the parameter σ (eq 112 in ref 19) is -7.5 kcal mol^{-1}, and the value of the entropy is -12 kcal mol^{-1} K^{-1}. Indeed, the quantitative agreement between both models is very good.

B. Conformational Properties. Let us now proceed to study the conformational properties of the model by analyzing the behavior of the fraction of the polymer in the helical conformation as a function of temperature. This is shown in Figure 8 for six chain lengths. Observe that this quantity is close to one at low temperatures predicting helix formation, and it approaches zero at high temperatures where no helices are present. One important observation is the sigmoidal shape of the curves. This shape is a direct consequence of the cooperativity of the transition and is captured correctly by our minimal model. Furthermore, this result agrees on a qualitative level with predictions arising from other computer simulation studies on atomistic models,[23,26,33] theories,[9,11] and experimental observations.[34] Another important feature of this result is its dependence on chain length. As the chain length increases, the transition temperature increases until it reaches a limiting value. This behavior is in good agreement with the predictions from standard helix−coil transition theories[9] and can be easily explained using basic statistical mechanics arguments.[35]

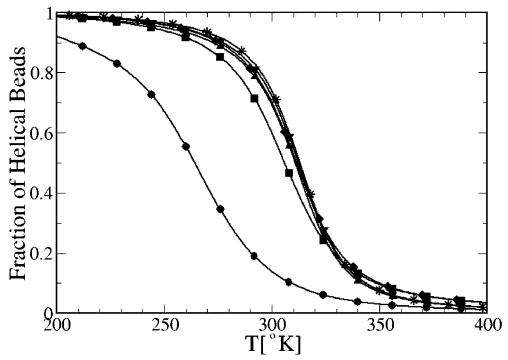

Figure 8. Plot of the fraction of the polymer in the helical conformation as a function of temperature for different chain lengths. The values of the parameters are $C = -1300$ K and $\eta = 0$ K. (●) $n = 10$, (■) $n = 20$, (◆) $n = 30$, (▲) $n = 40$, (▼) $n = 50$, (*) $n = 60$.

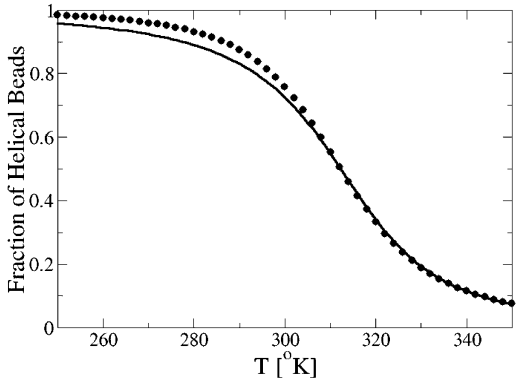

Figure 9. Plot of the fraction of the polymer in the helical conformation as a function of temperature (in K) for a chain with 50 beads: line (our result), circles (from Bloomfield's article).

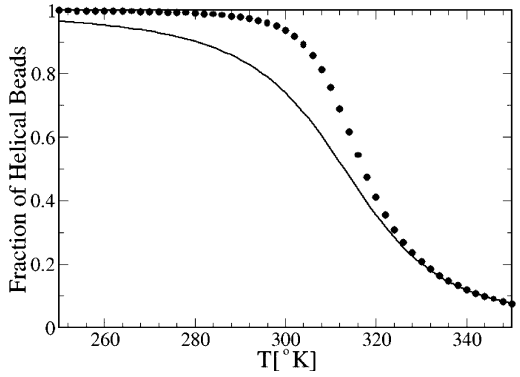

Figure 10. Plot of the fraction of the polymer in the helical conformation as a function of temperature (in K) for a chain with 60 beads: line (our result), circles (Nagai's model.).

Figures 9 and 10 show a comparison of the fraction of the polymer in the helical conformation predicted by our simulation study with the results obtained using two theoretical approaches. First, in Figure 9 we compare our result with the one obtained by Bloomfield, who considered the free ends of the polymer chain explicitly.[36] In this case the polymer has 50 beads ($n = 50$). The parameter η is equal to zero. In addition, the functional dependence of the parameter s (in Bloomfield's notation) on temperature was assumed to be of the form

$$s(T) = \exp\left(\frac{1300}{T} + \Delta S\right) \tag{11}$$

The optimal values of σ (in Bloomfield's notation) and ΔS are 0.02 and -4.163, respectively. It is important to point out that the value of σ ($= 0.02$) is less than one. This suggests that the cooperativity of the transition is included in our model to some extent even without incorporating the interfacial penalty explicitly ($\eta = 0$). This is the natural consequence of the restrictions introduced by the FRC model and the constraints on the dihedral angles together with the criterion used to determine the helical conformation. This conclusion is easy to understand if we follow the subsequent line of reasoning. Let us assume that we have a perfect helix. Now, we rotate one dihedral angle somewhere in the middle of the helix so that we break the helix into two shorter helices. The enthalpic cost to *create* the interface is $2C$ because, according to our determination of the helical conformation, the torsion depends on the positions of five consecutive beads (two consecutive dihedral angles). Now, consider the case where we remove a bead from one of the ends of a helical sequence where the interface *already* exists; then the enthalpic cost is only C. Note that in both cases the change in the entropy is the same. This implies that there is an extra enthalpy necessary to *create* a new interface and that its magnitude is C. The only way to capture this extra enthalpy necessary to *create* the interface within the framework of the traditional helix−coil transition theory is via the parameter σ, which must be less than one. This explains why σ must be different from one to describe our numerical results. Another interesting observation is the value of ΔS ($= -4.163$). It corresponds to the entropic cost that results from the FRC model and the constraints on the dihedral angles. The value of ΔS is very close to $-\ln 64 = -4.159$, which comes from the entropy change generated by a bead that changes its conformation from the random coil to the helical one.

We also compare our result for the fraction of the beads in the helical conformation with the one predicted by Nagai's model.[19] This is shown in Figure 10. To be consistent with the comparison presented in Figure 7, we used the same values for the parameters. We remind the reader that these parameters were optimized to provide a good quantitative agreement between both results for $\langle R^2 \rangle$. Thus, we regard the comparison shown in Figure 10 as very good since there are *no* adjustable parameters. Observe that the transition starts at the same temperature (when approached from high temperatures). Now, the width of the transition is not the same for both models. This is a consequence of the parameters used which can be optimized to obtain a very good quantitative agreement for the fraction of the polymer in the helical conformation. This would decrease the quality of the agreement shown in Figure 7. However, a compromise could be reached such that the descriptions of both quantities are acceptable. In addition, we remind the reader that Nagai's model does not include excluded-volume interactions and uses the freely jointed (not rotating) chain model. These differences might also contribute to the small quantitative differences observed in Figures 7 and 10. Still, the agreement is very good.

Figures 11 and 12 provide more insight into the mechanism behind the helix−coil transition. For example, Figure 11 shows the average number of helical *domains* as a function of temperature for chains of different lengths. Observe that for short chains ($n = 10$) the average number of helical domains is always less than one, while for long chains, this average is larger than one near the transition temperature. These results are in good qualitative agreement with the original results of Lifson and Roig[11] and indicate that short chains undergo the helix−coil transition by unwinding from the ends while long chains break into multiple helical domains near the transition temperature. Further insight is provided by Figure 12 where we plot the average length of a helical domain as a function of temperature. This figure clearly shows that, on average, the length of a helical domain decreases in a monotonic manner when the temperature is increased in agreement with the results shown in ref 11.

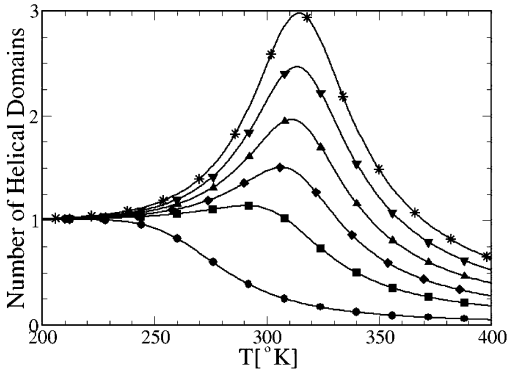

Figure 11. Plot of the average number of helical domains as a function of temperature for different chain lengths. The values of the parameters are $C = -1300$ K and $\eta = 0$ K. (●) $n = 10$, (■) $n = 20$, (◆) $n = 30$, (▲) $n = 40$, (▼) $n = 50$, (*) $n = 60$.

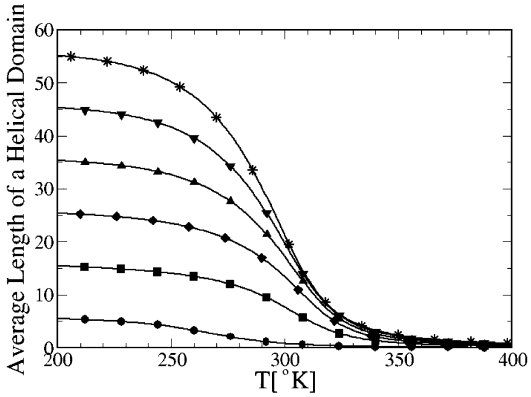

Figure 12. Plot of the average length of a helical domain as a function of temperature for different chain lengths. The values of the parameters are $C = -1300$ K and $\eta = 0$ K. (●) $n = 10$, (■) $n = 20$, (◆) $n = 30$, (▲) $n = 40$, (▼) $n = 50$, (*) $n = 60$.

C. Thermodynamic Properties. We start the study of the thermodynamic properties of the model with the evaluation of the entropy of the system. Figure 13 shows the entropy (in units of Boltzmann constant) as a function of temperature for chains of different lengths. The first observation is that the entropy increases with increasing temperature as expected from the second law of thermodynamics and approaches zero when the temperature approaches absolute zero, in agreement with the third law of thermodynamics. Moreover, it is independent of chain length for low enough temperatures. This is the natural consequence of the formation of helices at low temperatures because the number of degrees of freedom of a helix is independent of its length. Furthermore, Figure 14 shows the dependence of entropy on chain length in the high-temperature region. Observe that our model predicts a linear dependence of the entropy on the number of beads as it should be

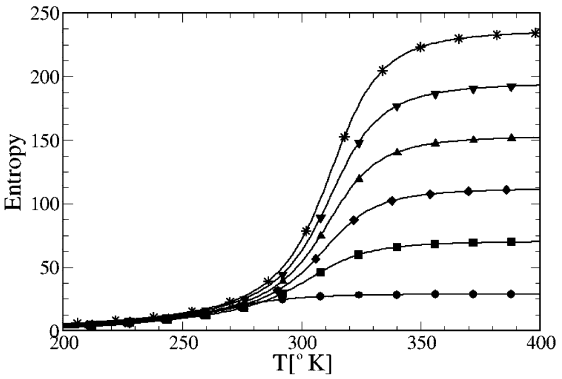

Figure 13. Plot of the entropy as a function of temperature for different chain lengths. The values of the parameters are $C = -1300$ K and $\eta = 0$ K. (●) $n = 10$, (■) $n = 20$, (◆) $n = 30$, (▲) $n = 40$, (▼) $n = 50$, (*) $n = 60$.

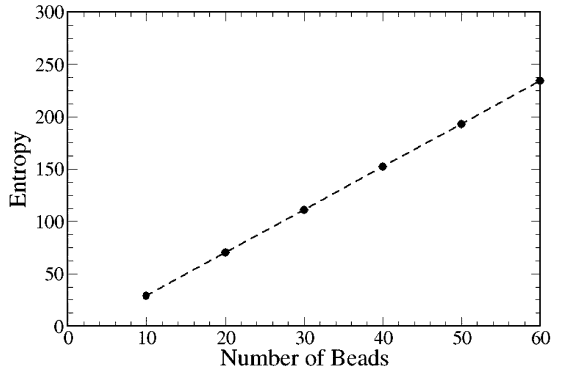

Figure 14. Plot of the entropy as a function of chain length at high temperatures.

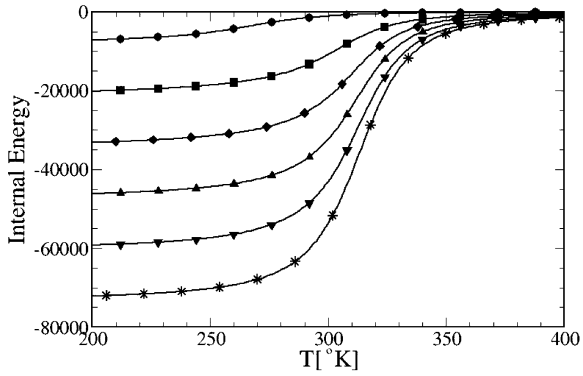

Figure 15. Plot of the internal energy as a function of temperature for different chain lengths. The values of the parameters are $C = -1300$ K and $\eta = 0$ K. (●) $n = 10$, (■) $n = 20$, (◆) $n = 30$, (▲) $n = 40$, (▼) $n = 50$, (*) $n = 60$.

because entropy is an extensive thermodynamic variable.

Figures 15 and 16 show the same plots for the internal energy (in kelvin). Figure 15 shows the dependence on temperature for different chain lengths. The internal energy increases as the temperature is raised and reaches the asymptotic value of zero at high temperatures. This is a consequence of using the random coil conformation as our reference state. It is relevant to note that the predicted functional dependence on temperature agrees on a qualitative level with recent predictions arising from the Zimm−Bragg theory which were used to describe experimental data.[37] In addition, the low-temperature region clearly shows that long chains are more stable than short ones since their

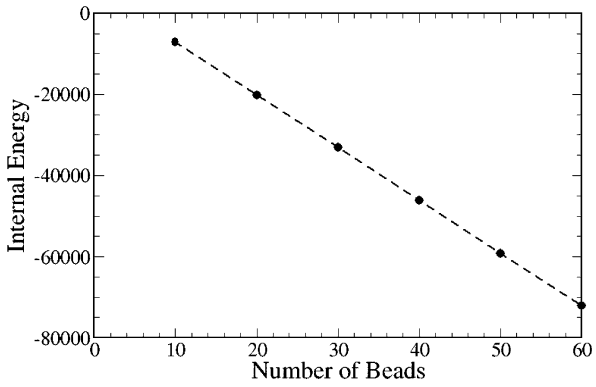

Figure 16. Plot of the internal energy as a function of chain length at low temperatures.

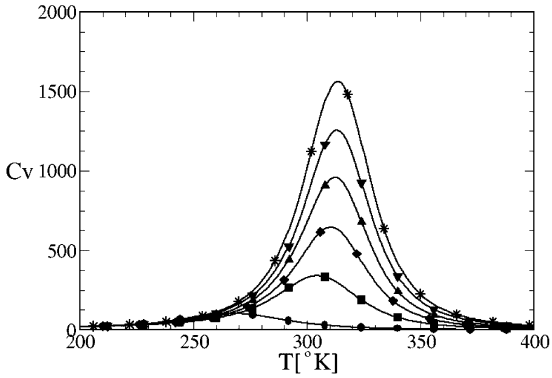

Figure 17. Plot of the heat capacity as a function of temperature for different chain lengths. The values of the parameters are $C = -1300$ K and $\eta = 0$ K. (●) $n = 10$, (■) $n = 20$, (◆) $n = 30$, (▲) $n = 40$, (▼) $n = 50$, (*) $n = 60$.

internal energy is lower. Figure 16 shows the dependence of the internal energy on chain length for the low-temperature region. As in the case of the entropy, the internal energy is a linear function of the number of beads, in agreement with the fact that it is an extensive thermodynamic variable.

Figure 17 shows the heat capacity as a function of temperature for polymers with different chain lengths. This figure shows that an increase in the length of the polymer increases the height of the peak and shifts the transition temperature toward higher values until it saturates at temperatures close to 313 K for large values of n. The temperature at which transition saturates depends on the ratio $C/\Delta S$. In addition, the width of the transition at half-height decreases monotonically with increasing chain length until it reaches a *limiting nonzero* value. This is in agreement with the fact that the helix−coil transition, as predicted by the Zimm−Bragg theory, is not a true thermodynamic transition. Figure 18 shows the height of the peak as a function of the number of beads. The relationship is linear in agreement with the fact that the heat capacity is an extensive thermodynamic variable. Moreover, the results shown in Figure 17 also agree with atomistic simulations of polyalanine[26] on a qualitative level.

D. Effect of the Interfacial Penalty. We now consider the effect of the interfacial penalty. For this purpose, we keep the length of the chain fixed ($n = 60$) and vary the parameter η. Figures 19, 20, and 21 show three different properties: $\langle R_g^2 \rangle$, the fraction of helical beads, and the heat capacity as a function of temperature for different values of the parameter η. Observe that all these plots show the same effect: the higher

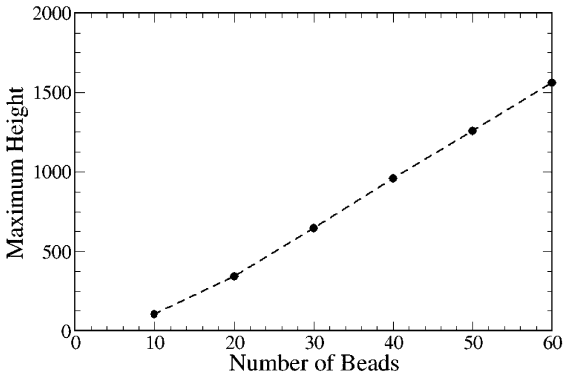

Figure 18. Plot of the maximum height of the heat capacity as a function of chain length.

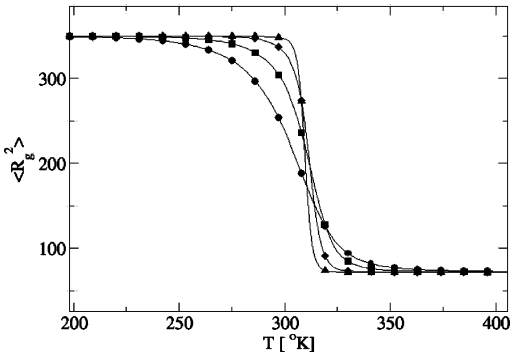

Figure 19. Plot of $\langle R_g^2 \rangle$ as a function of temperature for different values of the interfacial penalty. The values of the parameters are $C = -1300$ K and $n = 60$. (●) $\eta = 0$ K, (■) $\eta = 200$ K, (◆) $\eta = 600$ K, and (▲) $\eta = 1000$ K.

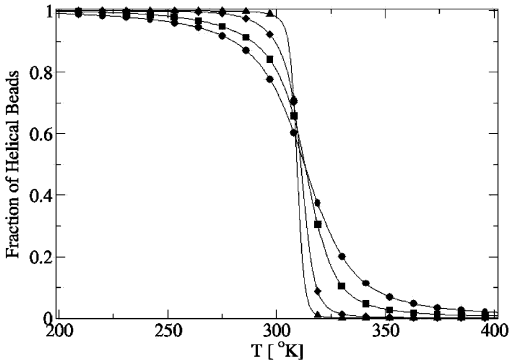

Figure 20. Plot of the fraction of the polymer in the helical conformation as a function of temperature for different values of the interfacial penalty. The values of the parameters are $C = -1300$ K and $n = 60$. (●) $\eta = 0$ K, (■) $\eta = 200$ K, (◆)$\eta = 600$ K, and (▲) $\eta = 1000$ K.

the interfacial penalty, the narrower the transition region. In other words, as the interfacial penalty increases, the helix−coil transition approaches the *all-to-none* transition originally proposed by Schellman.[35] This is the natural consequence of hindering those conformations with many helical domains which are very expensive in energy. Therefore, the chain prefers to go from the perfect helix to the random coil by avoiding those conformations that require the formation of interfaces.

E. Proposed Minimal Model. The results shown in the previous paragraphs suggest that the proposed minimal model is capable of describing all the properties characteristic of the helix−coil transition. Consequently, we can use the concepts behind the proposed minimal model to construct a *phenomenological* field-theoretic

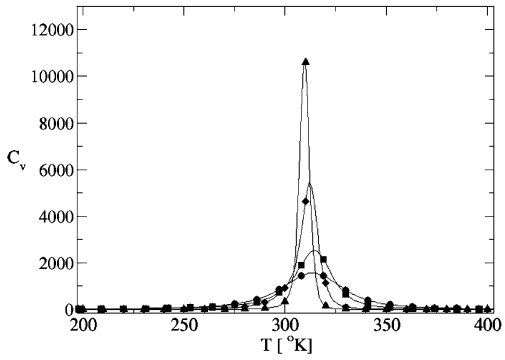

Figure 21. Plot of the heat capacity as a function of temperature for different values of the interfacial penalty. The values of the parameters are $C = -1300$ K and $n = 60$. (●) $\eta = 0$ K, (■) $\eta = 200$ K, (◆) $\eta = 600$ K, and (▲) $\eta = 1000$ K.

Hamiltonian of the Edwards type[38] that can describe the helix−coil transition of wormlike polymers. Such a Hamiltonian might be useful for the development of new theories for more complex systems of current interest like hydrogels of diblock copolypeptides[27] or networks of helix-forming polymers.[28]

We start by writing the statistical weight suggested by our simulation studies in the discrete form

$$\exp\left(-\beta C\sum_{i=2}^{n-2}\delta_{\Delta_i,\Delta_0} - \beta\eta\sum_{i=3}^{n-2}(\Delta_i - \Delta_{i-1})^2(\delta_{\Delta_i,\Delta_0} + \delta_{\Delta_{i-1},\Delta_0})\right) \times \text{geometrical constraints} \quad (12)$$

where β is the Lagrange multiplier $1/T$, T being the absolute temperature, C is the energy difference between the helical and random coil conformations for a single bead, δ is Kronecker's delta, Δ_i is the value of the torsion on the ith bead, Δ_0 is the torsion of the perfect helix, n is the number of beads in the chain, and η is the energy penalty for the presence of interfaces.

The first term in the exponential is the contribution arising from all those beads in the helical state. Observe that *only* those beads whose torsions are equal to the one of the perfect helix contribute to the summation. This condition is imposed by the Kronecker's delta inside the summation. Moreover, the contribution of each bead is the energy C. The second term is the contribution arising from the interfaces between helical and random coil domains. Observe that if the ith and $(i - 1)$th beads are in the helical conformation, then the square term in the sum is zero because both beads have the same torsion. Therefore, this term does not contribute if both consecutive beads are part of a helical domain. Similarly, if both beads are in the random coil conformation, then the Kronecker deltas will be zero because the torsions are not equal the one of the perfect helix. Consequently, the second term is not zero only when one of the beads is in the helical conformation while the other one is part of a random coil domain. The last contribution to eq 12 arises from the geometrical constraints. Explicitly, these constraints are two: first, the Kuhn length is fixed for all the bond vectors, and second, the bond angles are fixed. From a mathematical perspective, these two geometrical constraints can be realized using two Dirac delta distributions. We do not show the mathematical expressions of these two con-

straints in eq 12 because we are more interested in the continuous limit that we describe below.

We now proceed to take the continuous limit of eq 12 which allows us to define a field-theoretic Hamiltonian for the helix−coil transition, called H_{hc}, as follows:

$$\exp(-\beta H_{hc}) = \exp\left(-\beta\gamma\int_0^L dx\ \delta(\Delta(x)-\Delta_0)\times \left\{1+\mu\left(\frac{d\Delta(x)}{dx}\right)^2\right\}\right)\delta((\tau(x))^2-1)\delta\left(\left(\frac{d\tau(x)}{dx}\right)^2-\kappa_0^2\right)\times \delta\left(\Delta(x)-\frac{\tau(x)}{\kappa_0^2}\left(\frac{d\tau(x)}{dx}\frac{d^2\tau(x)}{dx^2}\right)\right) \quad (13)$$

Let us be more explicit about the derivation of this Hamiltonian from the discrete model. For this purpose, we start with the exponential which is the continuous version of the exponential in eq 12. First, we multiply and divide the argument of the exponential in eq 12 by the length of the bond vector, l_K, and then we take the limit $l_K \to 0$ such that $nl_K = L$ (the contour length of the chain), then we can write

$$\beta C\sum_{i=2}^{n-2} l_K \frac{\delta_{\Delta_i,\Delta_0}}{l_K} \to \beta\gamma\int_0^L dx\ \delta(\Delta(x)-\Delta_0) \quad (14)$$

where the parameter C has been replaced by its continuous counterpart γ, the summation becomes an integral over the arc of length parameter x, and the Kronecker delta (divided by l_K) has been replaced by the Dirac delta distribution. In this expression, $\Delta(x)$ is the torsion at location x along the continuous curve that represents the polymer chain and Δ_0 is the torsion of the perfect helix.

We also multiply and divide the second term in the exponential of eq 12 by l_K^3 and take the limit $l_K \to 0$ such that $nl_K = L$; then the second term can be written as follows

$$(\eta l_K^2)\sum_{i=3}^{n-2} l_K\left(\frac{\Delta_i-\Delta_{i-1}}{l_K}\right)^2\left(\frac{\delta_{\Delta_i,\Delta_0}}{l_K}+\frac{\delta_{\Delta_{i-1},\Delta_0}}{l_K}\right)\to \mu\int_0^L dx\left(\frac{d\Delta(x)}{dx}\right)^2\delta(\Delta(x)-\Delta_0) \quad (15)$$

where the summation and the Kronecker's deltas have been replaced by the integral and the Dirac delta, respectively, like in eq 14. Moreover, the square term involving the difference between the torsions of beads i and $i-1$ becomes the square of the derivative of the torsion with respect to the arch of length parameter. Finally, μ is the limiting value of $2\eta l_K^2$ when l_K goes to zero.

We have also written the explicit form of the geometric constraints in eq 13. Let us describe each of them. The first Dirac delta arises from the fact that the length of the bond vectors was kept constant during the simulation study. This constraint has important consequences for different physical properties of the model (e.g., the force−elongation relationship). To implement this constraint on the continuous model, we have to use the *local inextensibility constraint* also employed in the wormlike chain model.[32] This constraint is always written as a Dirac delta of the square of the tangent vector, $\tau(x)$, minus 1 where $\tau(x)$ is the vector tangent to the curve that represents the polymer chain. The second geometric constraint used in our simulation study is related to the bond angles. These angles were kept constant during the simulation. Observe that if we define the bond angle as θ, then the following equality is true

$$\left(\frac{2\cos\left(\frac{\theta}{2}\right)}{l_K}\right)^2 = \left(\frac{\tau_{i+1}-\tau_i}{l_K}\right)^2 \quad (16)$$

where τ_i is the bond vector from the ith bead to the $i+1$. Note that the second parenthesis is the mathematical definition of curvature for a discrete representation of the chain. Let us call the curvature of the perfect helix κ_0, which is constant. Thus, when we take the continuous limit of the discrete model, κ_0 must not be altered. This can be accomplished as follows

$$\lim_{l_K\to 0}\frac{2\cos\left(\frac{\theta}{2}\right)}{l_K} = \kappa_0 \quad (17)$$

which implies that as l_K goes to zero, θ approaches π such that the limit, eq 17, is satisfied. Observe that if κ_0 is zero, then the angle θ is must be equal to π for any value of the Kuhn length. This implies that the configuration of the polymer is rodlike. Consequently, the torsion becomes an ill-defined quantity, and our simulation study and theoretical model break down. However, the objective of this work is to model helical polymers. These polymers are stabilized by the formation of hydrogen bonds between residues; if the polymer is a rodlike polymer, then the residues cannot form hydrogen bonds and helices do not form. Thus, our model is not expected to capture the limit of rodlike polymers. Finally, the third Dirac delta is the definition of the torsion in terms of the tangent vector.

Observe that the first two deltas imply that the tangent vector is orthogonal to its first-order derivative which is orthogonal to the second-order derivative. These geometric constraints can be used to simplify the form of eq 13. We leave the analysis of this Hamiltonian for a future article. However, we would like to emphasize that this Hamiltonian is a direct consequence of our simulation study.

Conclusions

In this article we have explored a novel approach to the simulation of the helix−coil transition of wormlike polymers. Our approach builds on the traditional concepts of helix−coil transition theory and adds the geometrical property of torsion of a curve. This new parameter allows us to bridge between the conformational and configurational properties of the polymer chain. Therefore, real-space properties like the radial distribution function can be calculated in addition to the traditional conformational properties like the fraction of the polymer in the helical conformation. All these properties are calculated from the same model. In addition, the use of torsion to determine the conformational state of each bead is equivalent to the use of two consecutive dihedral angles. Therefore, the cooperativity of the helix−coil transition is taken into account explicitly in this model.

We have showed that the use of torsion in the criterion that determines the conformational state of each bead leads to results that agree with predictions arising from other computational, theoretical, and experimental studies on a qualitative and quantitative level. Therefore, this model might be used to study systems where the helical structure of the polymer is important but the atomistic details are not. One example of this is the case of networks of helical polymers where the atomistic details are not so relevant for the mechanical and thermodynamic properties, but the helical structure of the polymer must be described correctly.

Another area where we believe our model might have interesting consequences is the one of polyelectrolytes and polyampholytes. In these fields, the possibility of helix formation will add another degree of freedom to these already very challenging systems. Therefore, we foresee an enrichment of the physics of these systems. For example, it would be very interesting to study how helix formation gets coupled and modifies the different scaling regimes predicted for polyelectrolytic systems or how helix formation couples to the counterion condensation mechanism. These and other possibilities are of current scientific interest and will be addressed in forthcoming articles.

Acknowledgment. This material is based upon work partially supported by the National Science Foundation under Grant CHE-0132278. Also, acknowledgment is made to the donors of the Petroleum Research Fund, administered by the American Chemical Society, for partial support of this research (PRF# 37051-G7) and The Ohio Board of Regents, Action Fund (Grant# R566).

References and Notes

(1) Pauling, L.; Corey, R. *J. Am. Chem. Soc.* **1950**, *72*, 5349. Pauling, L.; Corey, R. B.; Branson, H. R. *Proc. Natl. Acad. Sci. U.S.A.* **1951**, *37*, 205. Pauling, L.; Corey, R. B. *Proc. Natl. Acad. Sci. U.S.A.* **1951**, *37*, 235. Pauling, L.; Corey, R. B. *Proc. Natl. Acad. Sci. U.S.A.* **1951**, *37*, 251.
(2) Teramoto, A. *Prog. Polym. Sci.* **2001**, *26*, 667.
(3) Sayama, N.; Kida, K.; Norisuye, T.; Teramoto, A.; Fujita, H. *Polym. J.* **1972**, *3*, 538. Norisuye, T.; Misumi, K.; Teramoto, A.; Fujita, H. *Biopolymers* **1973**, *12*, 1533. Nishioka, N.; Maekawa, A.; Teramoto, A. *Biopolymers* **1978**, *17*, 665. Noudeh, G. D.; Taulier, N.; Chalikian, T. V. *Biopolymers* **2003**, *70*, 563.
(4) Green, M. M.; Lifson, S.; Teramoto, A. *Chirality* **1991**, *3*, 285. Green, M. M.; Khatri, C.; Peterson, N. C. *J. Am. Chem. Soc.* **1993**, *115*, 4941. Green, M. M.; Peterson, N. C.; Sato, T.; Teramoto, A.; Cook, R.; Lifson, S. *Science* **1995**, *268*, 1860.
(5) Yashima, E.; Matsushima, T.; Okamoto, Y. *J. Am. Chem. Soc.* **1997**, *119*, 6345. Maeda, K.; Okada, S.; Yashima, E.; Okamoto, Y. *J. Polym. Sci., Part A: Polym. Chem.* **2001**, *39*, 3180.
(6) Lee, A. T.; McHugh, A. J. *Biopolymers* **1999**, *50*, 589.
(7) Zozulya, V. N.; Nesterov, A. B.; Ryazanova, O. A.; Blagoi, Y. P. *Int. J. Biol. Macromol.* **2003**, *33*, 183.
(8) Read, M. J.; Burkett, S. L. *J. Colloid Interface Sci.* **2003**, *261*, 255. Wang, Y.; Chang, Y. C. *Macromolecules* **2003**, *36*, 6503. Wang, Y.; Chang, Y. C. *Macromolecules* **2003**, *36*, 6511. Sukhishvili, S. A.; Granick, S. *Langmuir* **2003**, *19*, 1980.
(9) Gibbs, J. H.; DiMarzio, E. A. *J. Chem. Phys.* **1959**, *30*, 271.
(10) Zimm, B. H.; Bragg, J. K. *J. Chem. Phys.* **1959**, *31*, 526.
(11) Lifson, S.; Roig, A. *J. Chem. Phys.* **1961**, *34*, 1963.
(12) Farago, O.; Pincus, P. *Eur. Phys. J. E* **2002**, *8*, 393.
(13) Scheraga, H. A.; Vila, J. A.; Ripoll, D. R. *Biophys. Chem.* **2002**, *101*−*102*, 255. Selinger, J. V.; Selinger, R. L. B. *Phys. Rev. E* **1997**, *55*, 1728.
(14) Zimm, B. H.; Rice, S. A. *Mol. Phys.* **1960**, *3*, 391.
(15) Tanaka, F. *Macromolecules* **2004**, *37*, 605.
(16) Doig, A. J. *Biophys. Chem.* **2002**, *101*−*102*, 281.
(17) Buhot, A.; Halperin, A. *Phys. Rev. Lett.* **2000**, *84*, 2160.
(18) Tamashiro, M. N.; Pincus, P. *Phys. Rev. E* **2001**, *63*, 021909.
(19) Nagai, K. *J. Chem. Phys.* **1961**, *34*, 887.
(20) Buhot, A.; Halperin, A. *Macromolecules* **2002**, *35*, 3238.
(21) Muthukumar, M. *J. Chem. Phys.* **1996**, *104*, 691.
(22) Paoletti, S.; Benegas, J. C.; Pantano, S.; Vetere, A. *Biopolymers* **1999**, *50*, 705.
(23) Hansmann, U. H. E.; Okamoto, Y. *J. Comput. Chem.* **1993**, *14*, 1333. Okamoto, Y.; Hansmann, U. H. E. *J. Phys. Chem.* **1995**, *99*, 11276. Alves, N. A.; Hansmann, U. H. E. *J. Phys. Chem. B* **2003**, *107*, 10284. Kemp, J. P.; Chen, Z. Y. *Phys. Rev. Lett.* **1998**, *81*, 3880.
(24) Wang, F.; Landau, D. P. *Phys. Rev. Lett.* **2001**, *86*, 2050.
(25) Rathore, N.; de Pablo, J. J. *J. Chem. Phys.* **2002**, *116*, 7225.
(26) Peng, Y.; Hansmann, U. H. E.; Alves, N. A. *J. Chem. Phys.* **2003**, *118*, 2374.
(27) Norwak, A. P.; Breedveld, V.; Pakstis, L.; Ozbas, B.; Pine, D. J.; Pochan, D.; Deming, T. J. *Nature (London)* **2002**, *417*, 424.
(28) Kutter, S.; Terentjev, E. M. *Eur. Phys. J. E* **2002**, *8*, 539.
(29) Abramowitz, M.; Stegun, I. A. *Handbook of Mathematical Functions with Formulas, Graphs and Mathematical Tables*; Dover Publications: New York, 1965.
(30) Budak, B. M.; Fomin, S. V. *Multiple Integrals, Field Theory and Series*; MIR Publishers: Moscow, 1973.
(31) Yan, Q.; de Pablo, J. J. *Phys. Rev. Lett.* **2003**, *90*, 035701.
(32) Wilhelm, J.; Frey, E. *Phys. Rev. Lett.* **1996**, *77*, 2581.
(33) Takano, M.; Nagayama, K.; Suyama, A. *J. Chem. Phys.* **2002**, *116*, 2219.
(34) Ackermann, T.; Ruterjans, H. *Ber. Bunsen-Ges. Phys. Chem.* **1964**, *68*, 850.
(35) Poland, D.; Scheraga, H. A. *Theory of Helix-Coil Transition in Biopolymers*; Academic Press: New York, 1970.
(36) Bloomfield, V. A. *Am. J. Phys.* **1999**, *67*, 1212.
(37) Kromhout, R. A.; Linder, B. *J. Phys. Chem. B* **2001**, *105*, 4987.
(38) Doi, M.; Edwards, S. F. *The Theory of Polymer Dynamics*; Clarendon Press: Oxford, England, 1986.

MA049338U